

CubeSat multi-band optical receiver for the Lunar Flashlight mission

Frankfurt, Germany- 17 May 2018

Quentin Vinckier¹, Karlton Crabtree², Megan Gibson³, Christopher Smith³, Udo Wehmeier¹, Paul O. Hayne⁴, R. Glenn Sellar¹

¹Jet Propulsion Laboratory, California Institute of Technology

²Photon Engineering LLC

³Sierra Lobo Inc.

⁴University of Colorado

Contact: vinckier@jpl.nasa.gov

- 1 Introduction
- 2 Instrument operation principle
- 3 Receiver optomechanical design
- 4 Conclusions and perspectives

NASA Strategic Knowledge Gaps: concentration and distribution of lunar volatiles, in particular water.

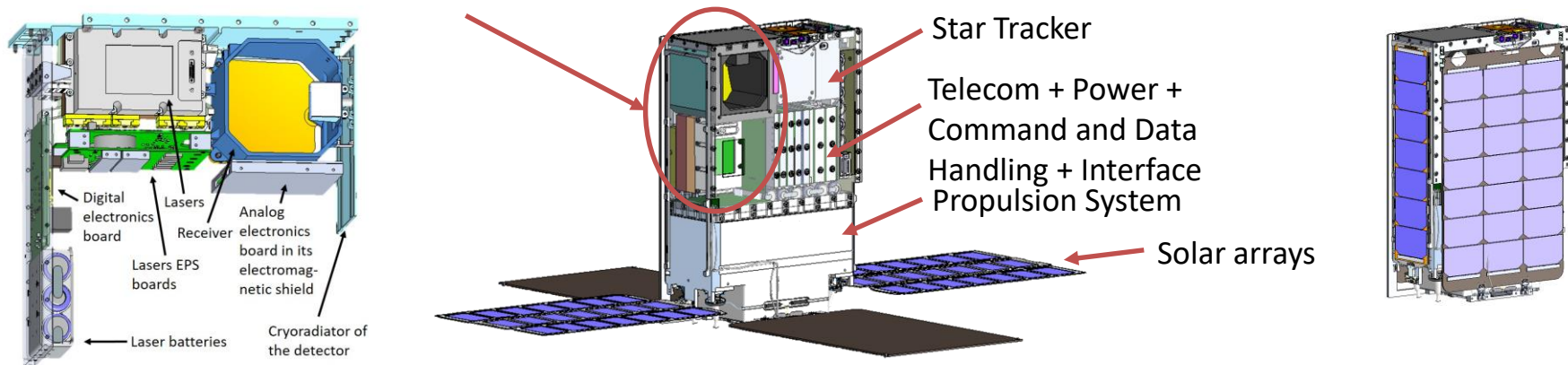
Background: strong indications of the presence of water ice in the Permanently Shadowed Regions (PSRs) of the lunar South Pole [1-4].

Lunar Flashlight goals:

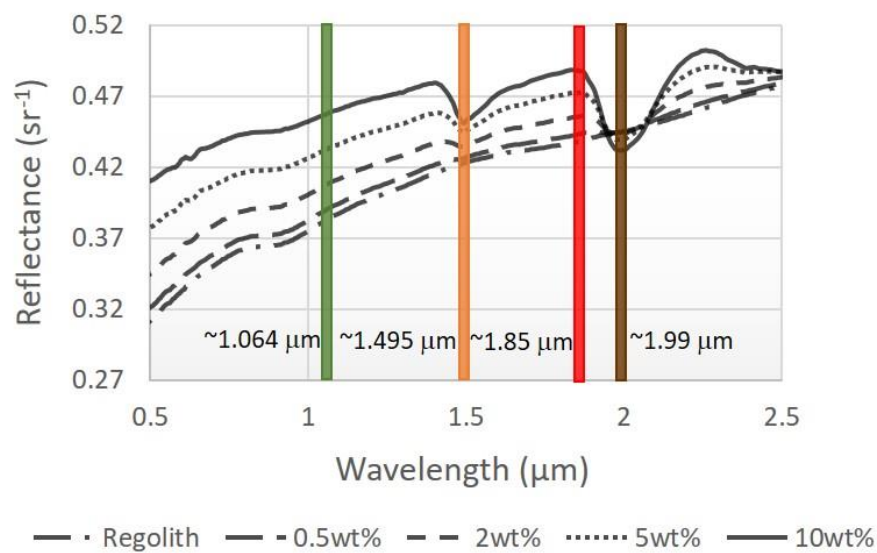
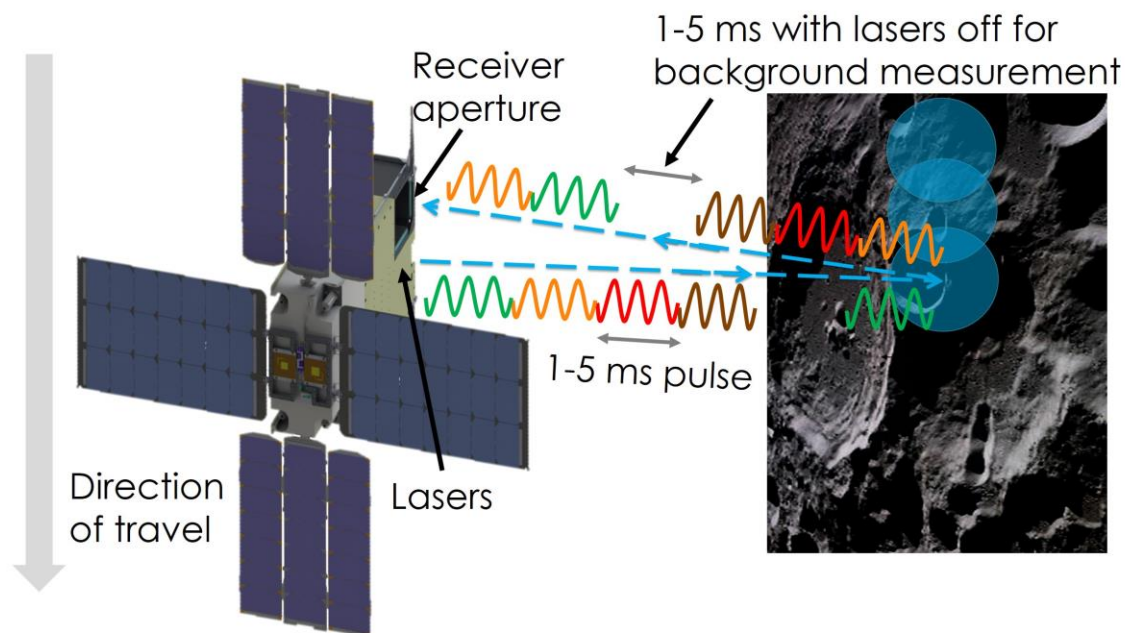
- ① measure water ice concentrations on the lunar South Pole above 0.5 weight %
- ② map water ice distribution with a resolution of 1-2 km

How : multi-band reflectometry from orbit.

Instrument: SWIR laser reflectometer



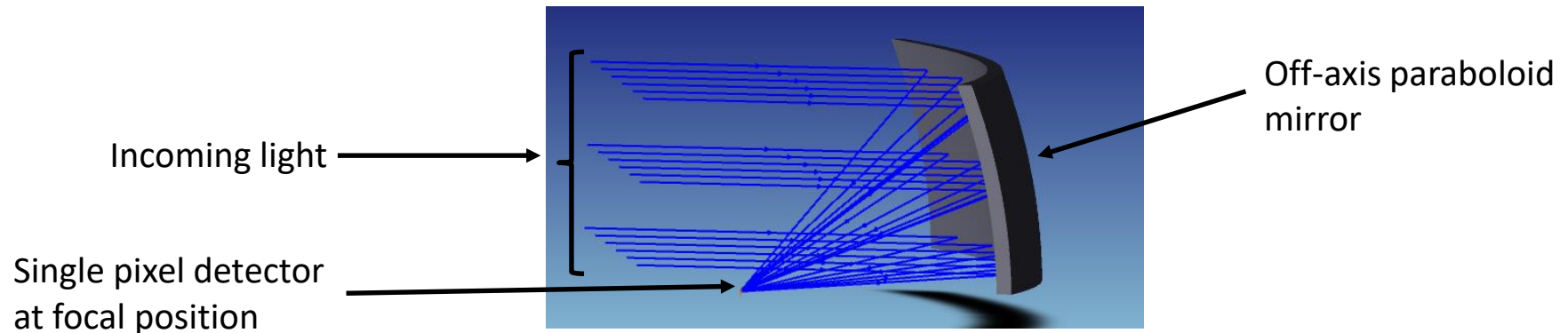
- [1] Hayne, P. O. et al., "Evidence for exposed water ice in the Moon's south polar regions from Lunar Reconnaissance Orbiter ultraviolet albedo and temperature measurements," *Icarus* 255, 58-69 (2015).
- [2] Thomson, B. J. et al., "An upper limit for ice in Shackleton crater as revealed by LRO Mini-RF orbital radar," *Geophysical Research Letters* 39(14) (2012).
- [3] Schwadron, N. A. et al., "Signatures of volatiles in the lunar proton albedo," *Icarus* 273, 25-35 (2016).
- [4] Fisher, E. A. et al., "Evidence for surface water ice in the lunar polar regions using reflectance measurements from the Lunar Orbiter Laser Altimeter and temperature measurements from the Diviner Lunar Radiometer Experiment," *Icarus* 292, 74-85 (2017).



[5] Cohen, B. A. et al., "Payload Design for the Lunar Flashlight Mission," Proc. Lunar and Planetary Science Conference 48, 1709 (2017).

[6] Vinckier, Q. et al., "System Performance Modeling of the Lunar Flashlight CubeSat Instrument", Proc. Lunar and Planetary Science Conference 49, 1030 (2018).

Receiver concept:



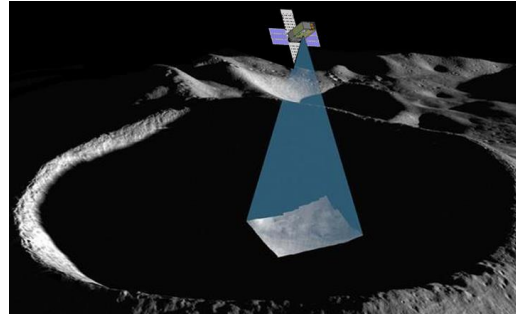
Design phases:

- 1 Selection of the mirror focal length and the detector active area diameter
- 2 Stray light analysis to minimize the background
- 3 Mechanical design

} Optical design

Mirror Focal Length (FL) and diameter (\emptyset) of the detector active area :

$$FOV = 2 \times \arctan \left\{ \frac{\emptyset}{2 \times FL} \right\}$$

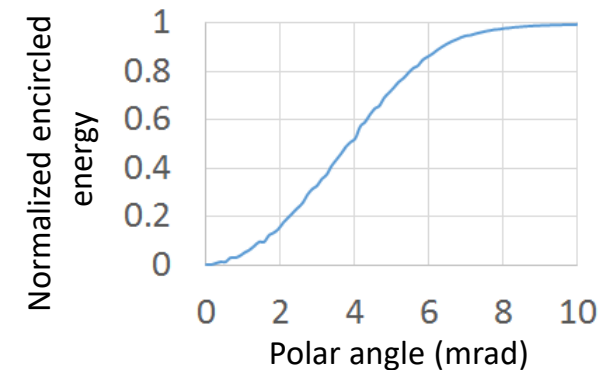
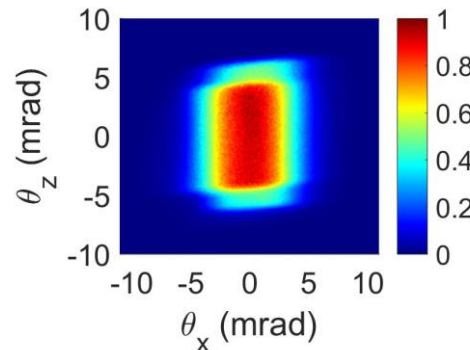


Driven factors:



Maximization of the lasers' photons detection efficiency

Laser beams divergence profile

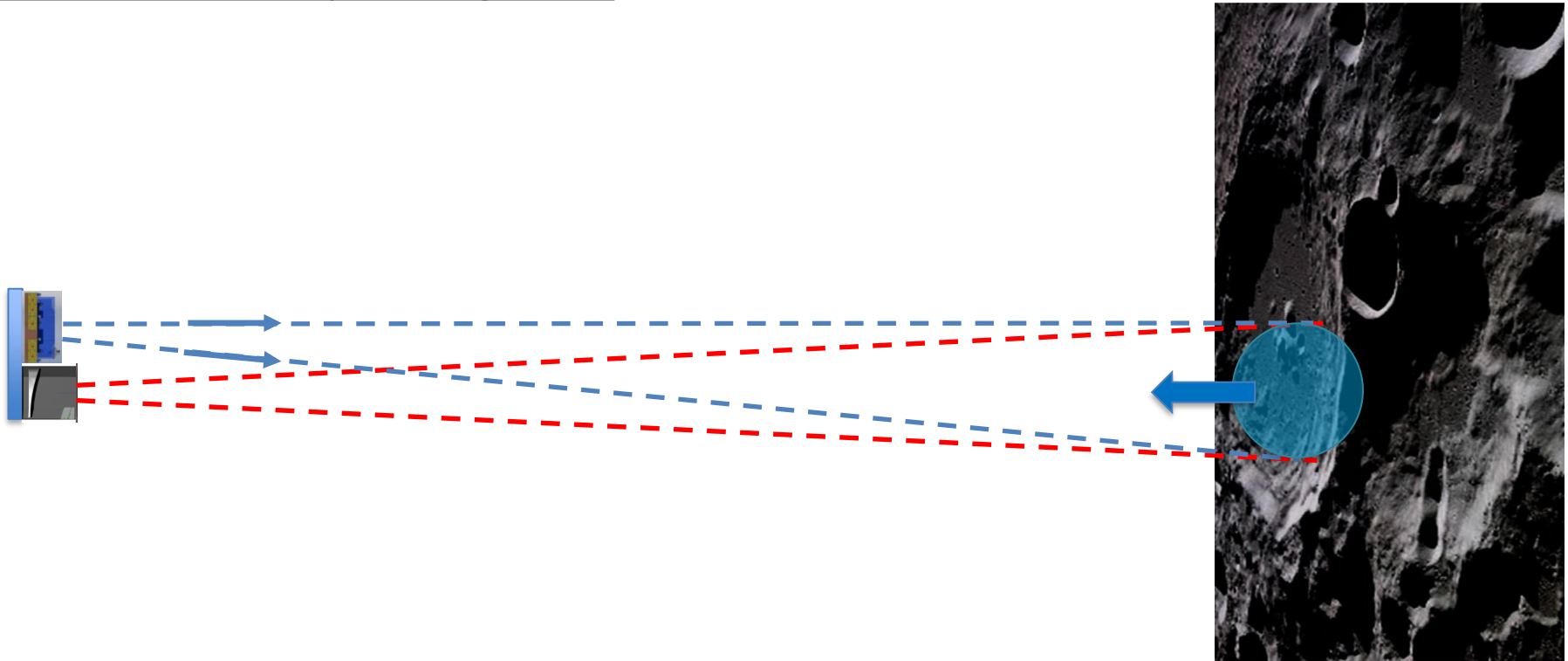


Minimization of the detected solar illumination of the Moon surface (background)

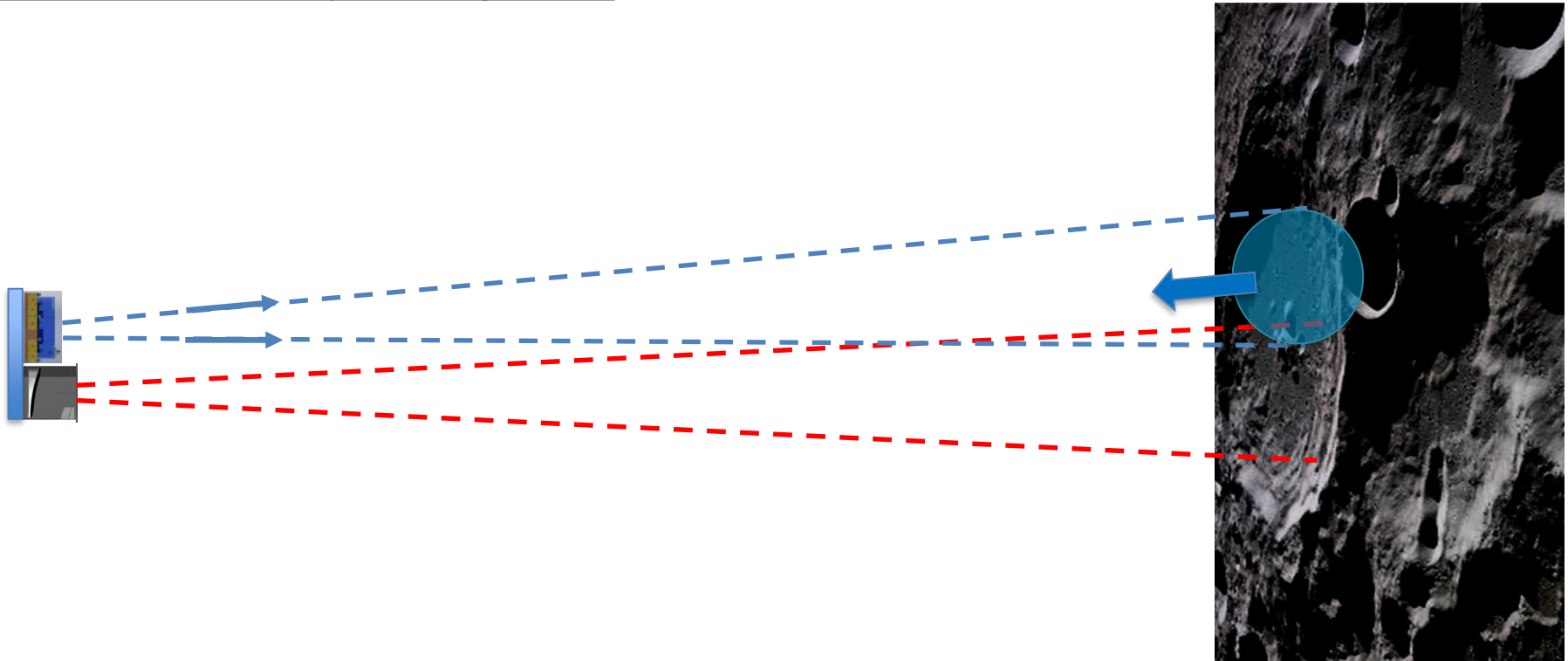


FOV margins to accommodate the laser-to-receiver pointing error budget

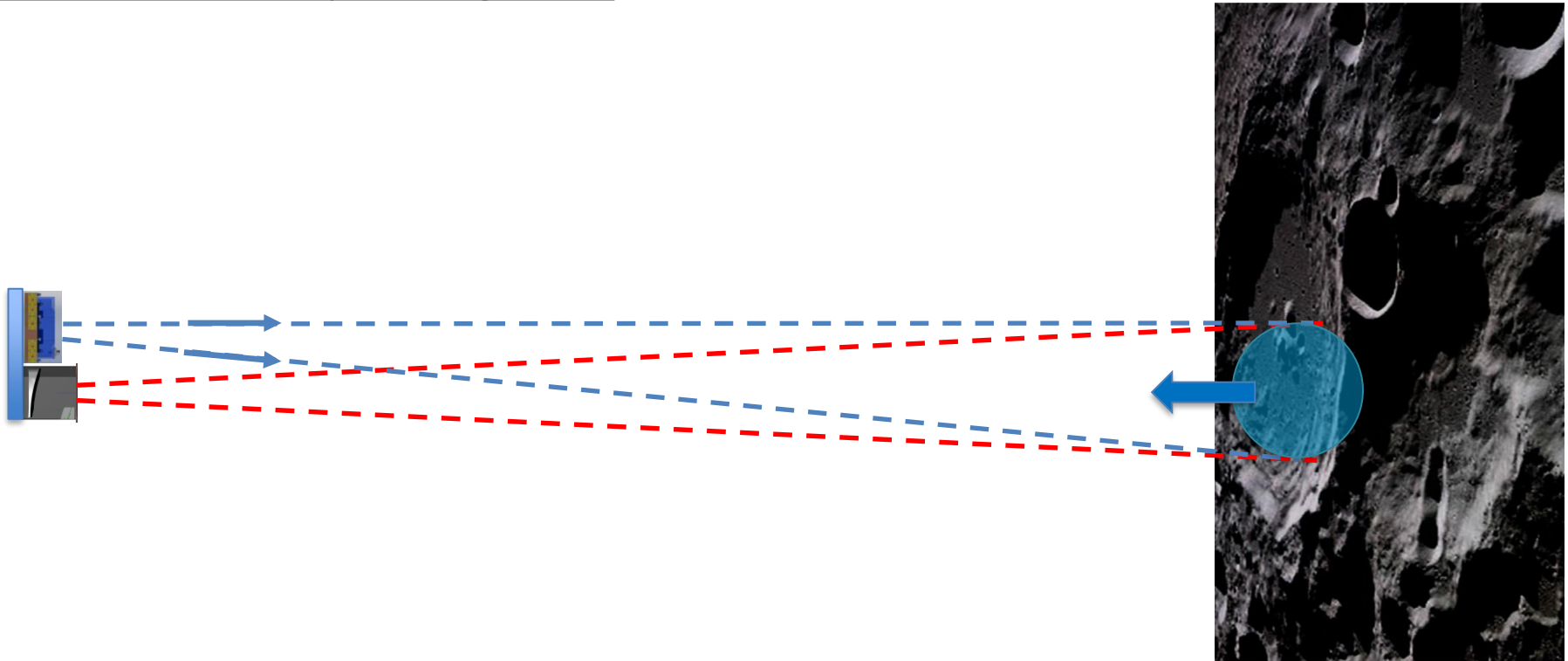
Laser-to-receiver pointing error



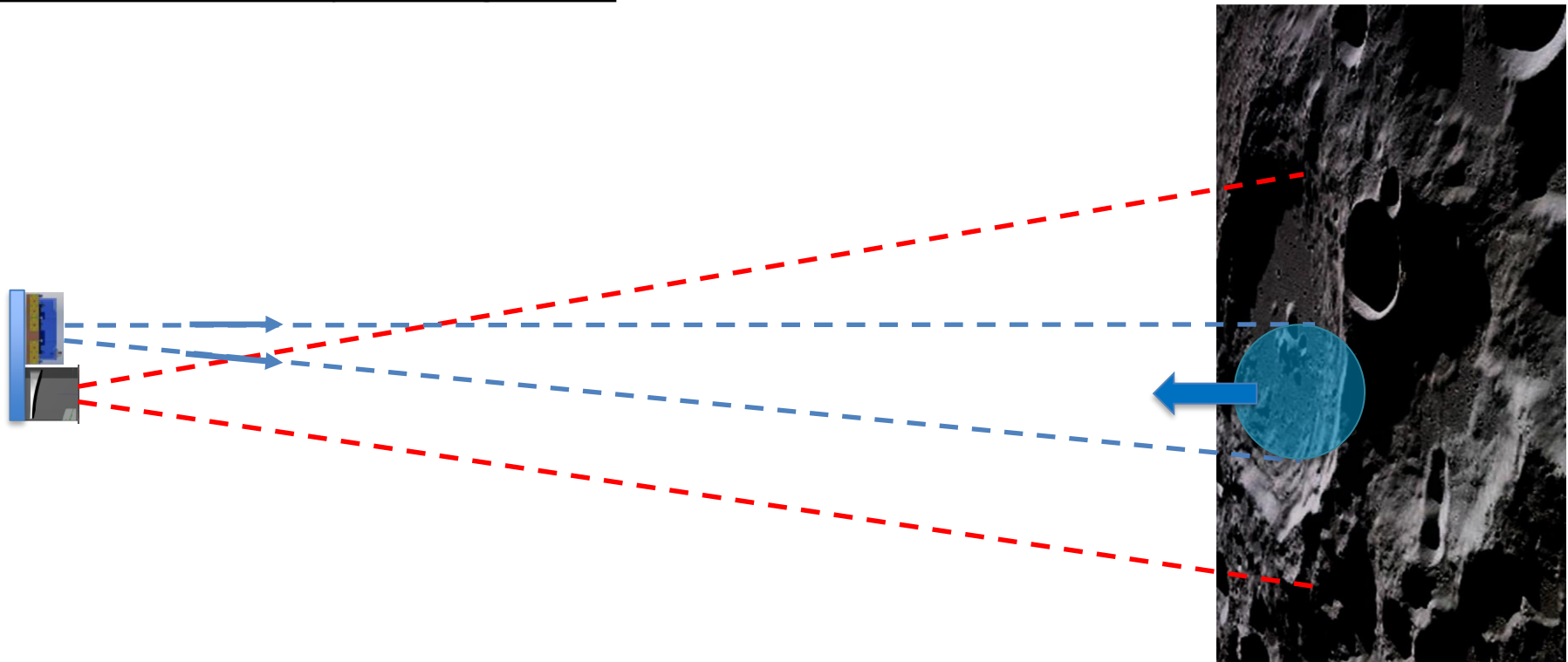
Laser-to-receiver pointing error



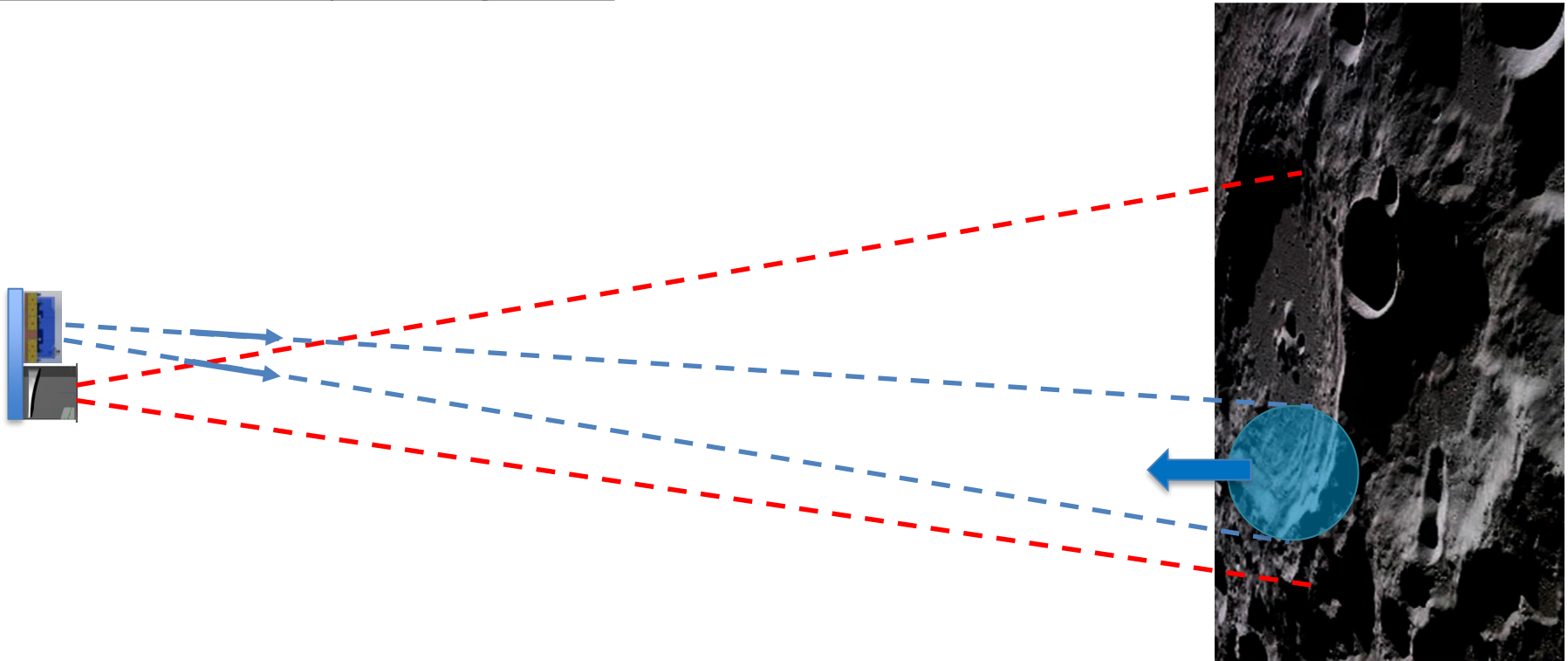
Laser-to-receiver pointing error



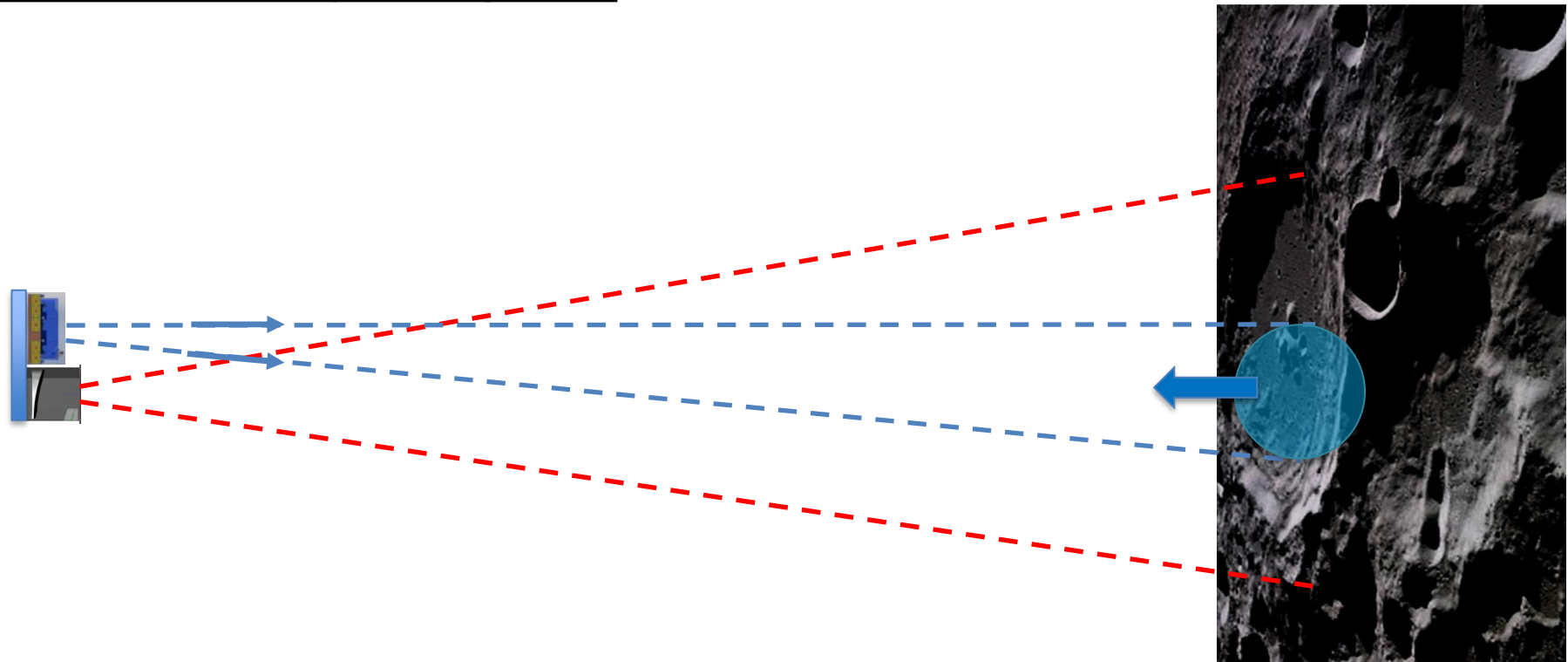
Laser-to-receiver pointing error



Laser-to-receiver pointing error



Laser-to-receiver pointing error

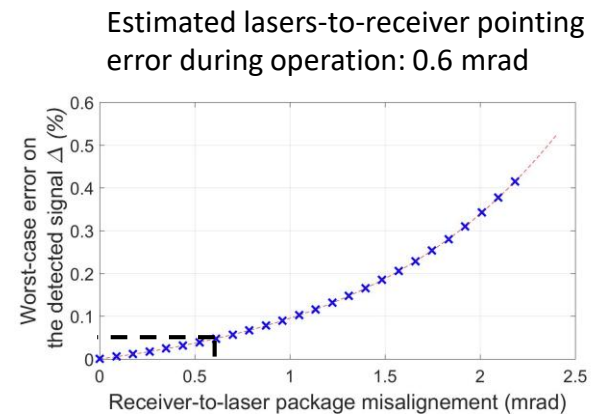
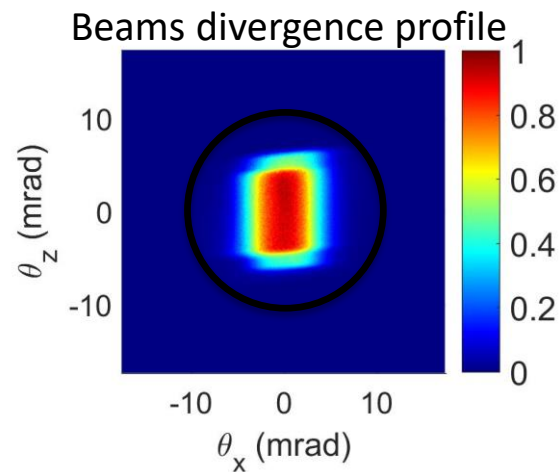
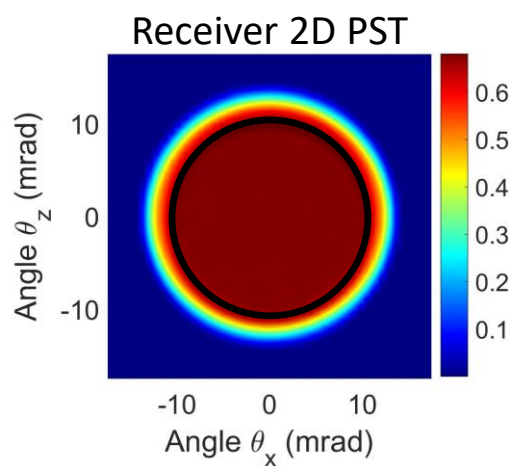


Our design:

$\phi = 2 \text{ mm}$

$FL = 70 \text{ mm}$

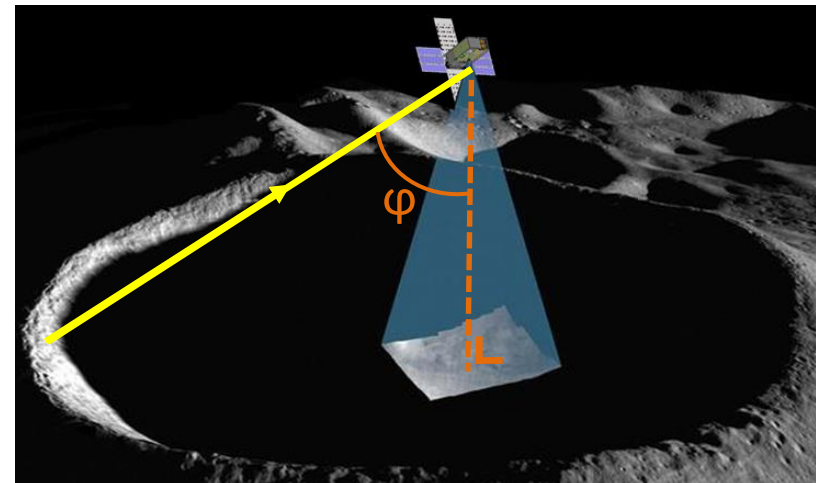
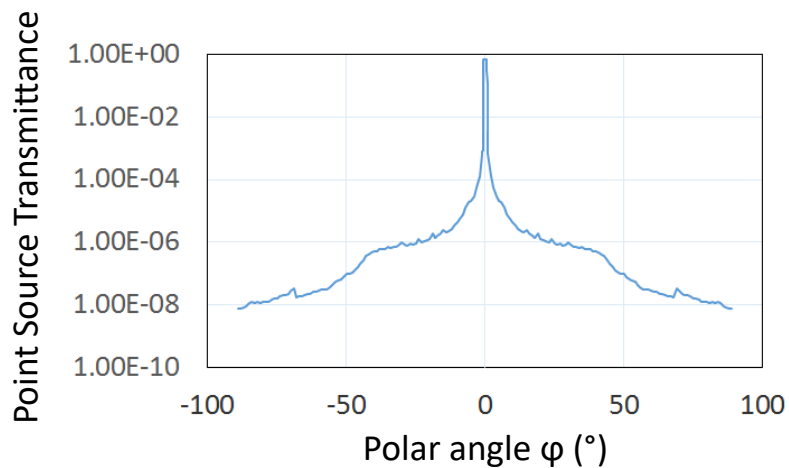
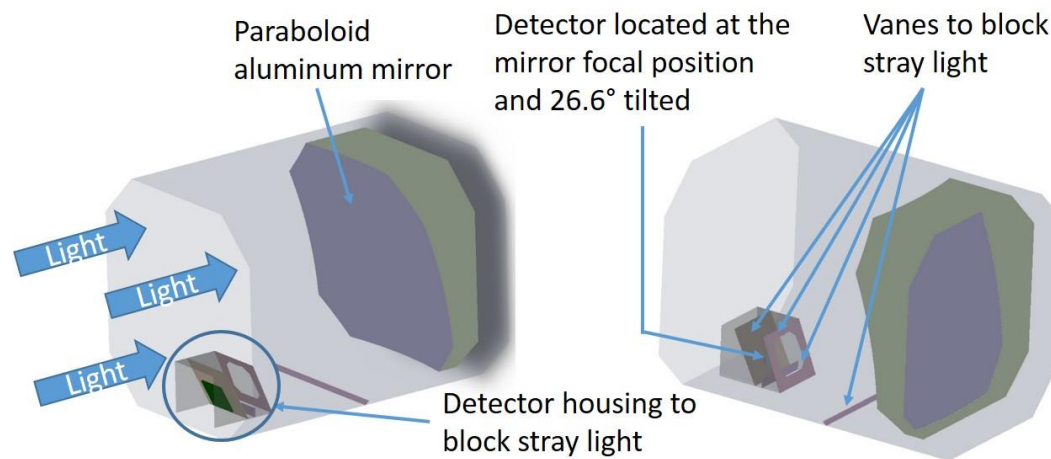
$FOV = 20 \text{ mrad}$



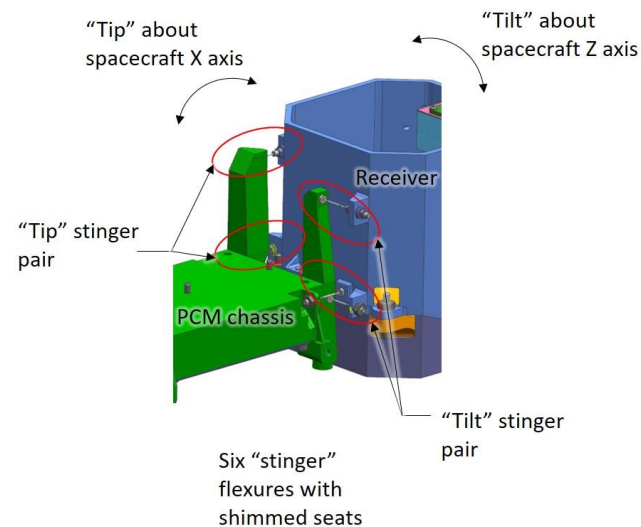
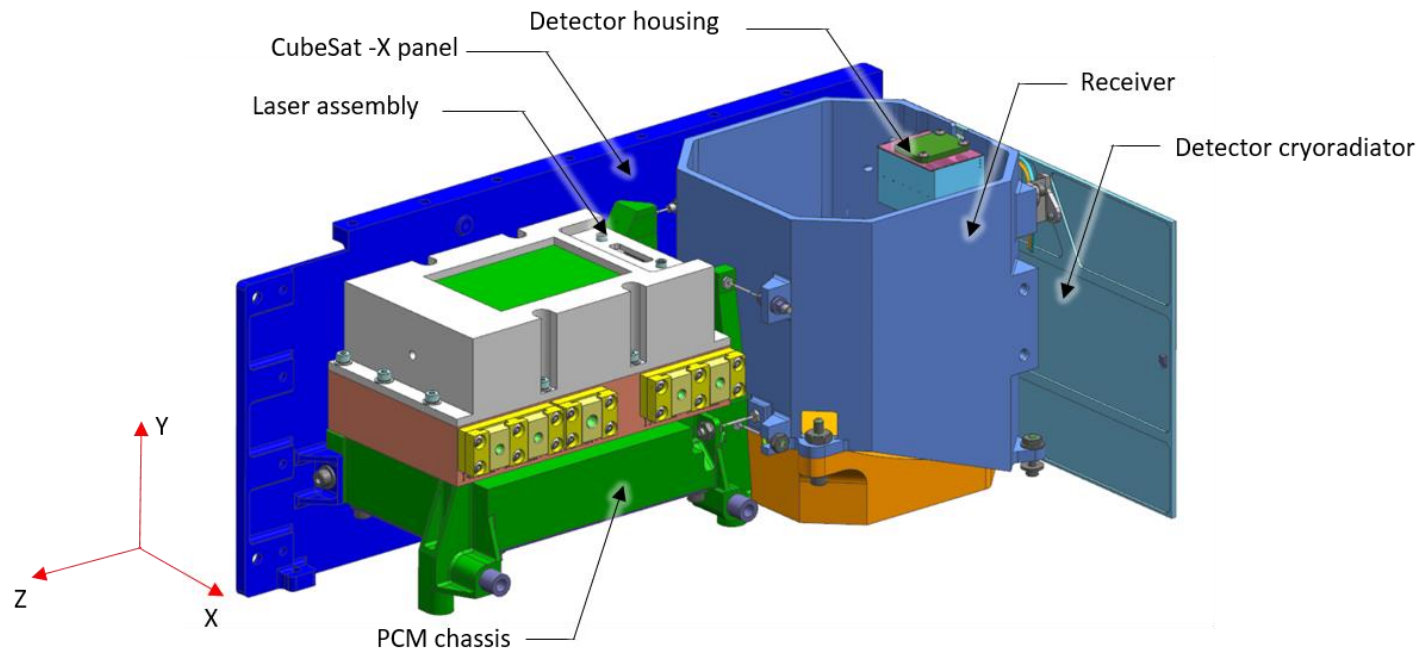
Stray light analysis:

➡ **Goal:** Minimization of the detected solar illumination of the Moon surface outside the receiver FOV

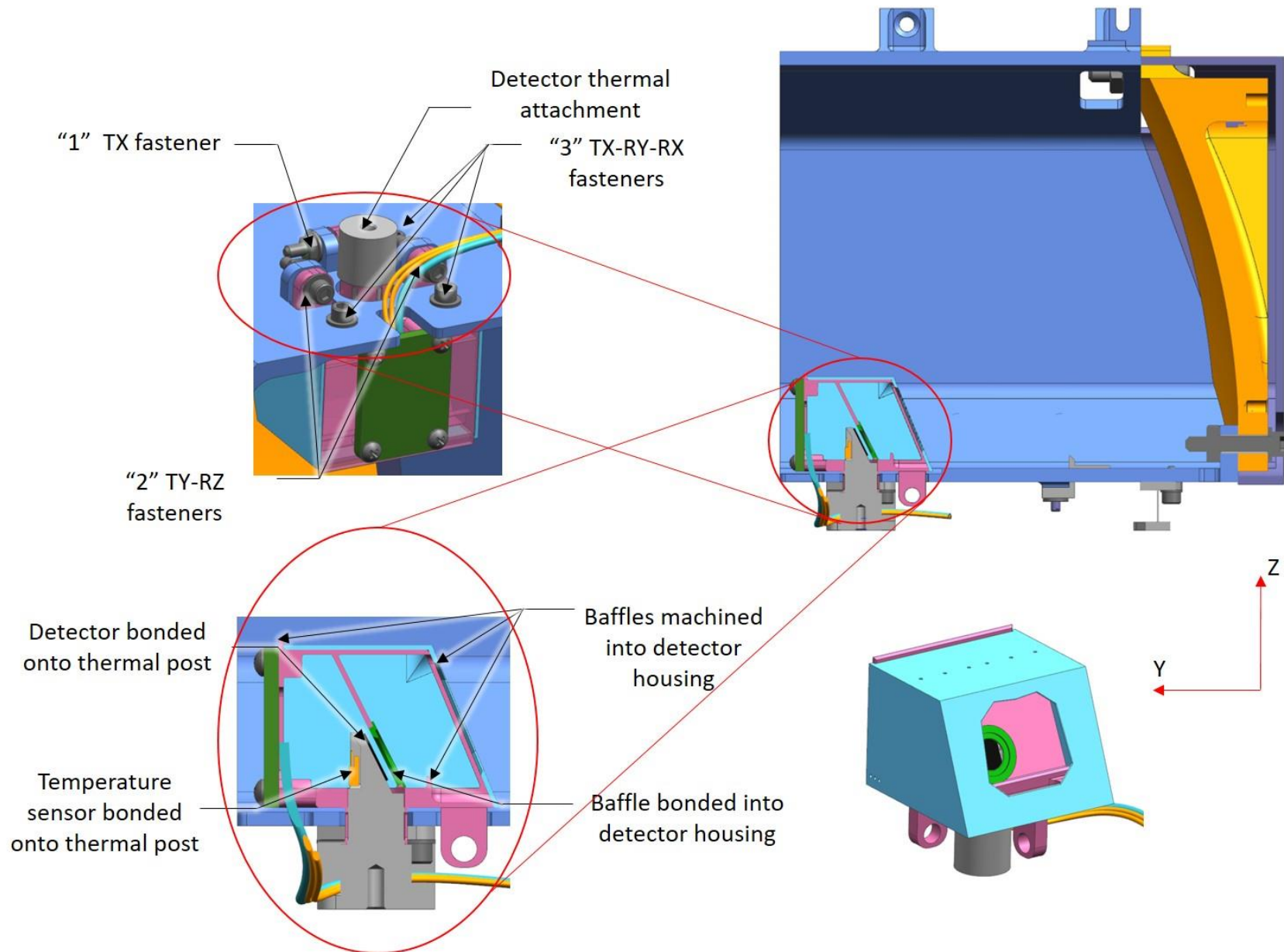
➡ **Optical design:**



Mechanical design:



Mechanical design:





Design of a SWIR optical receiver based on an aluminum paraboloid mirror focusing incoming light onto a single pixel detector.



Main challenge: design optimization (detector diameter, focal length, vanes/baffles) to minimize the overall uncertainty on the measurements.



Next steps: manufacture, calibration & characterization, integration to the CubeSat.



This will be one of the first instruments onboard a CubeSat performing science measurements beyond low Earth orbit and the first planetary mission to measure reflectance using active sources from orbit.



**Thank you for your
attention!**



Appendices



Stray light – Model limitations

- **This includes only 2 levels of scatter (any ray which attempts to scatter a 3rd time is stopped)**
 - This is not a major limitation, since the energy remaining in such a ray will be quite small
- **The number of rays incident on the system is approximately 2 rays per sq mm**
 - Since all relevant structures are at least 2.5mm in the smallest dimension, this should be adequate
- **BSDFs are always approximate, even well characterized surfaces like Z306 can vary by nearly a factor of two between various measurements**



- The PST is the ratio of the average detector irradiance to the incident irradiance, computed as a function of angle:

$$PST(\theta, \phi) = \frac{E_{det}(\theta, \phi)}{E_{inc}(\theta, \phi)} = \frac{E_{det}(\theta, \phi)}{P_{inc, norm} \cdot \cos(\theta) / A_{entrance}}$$

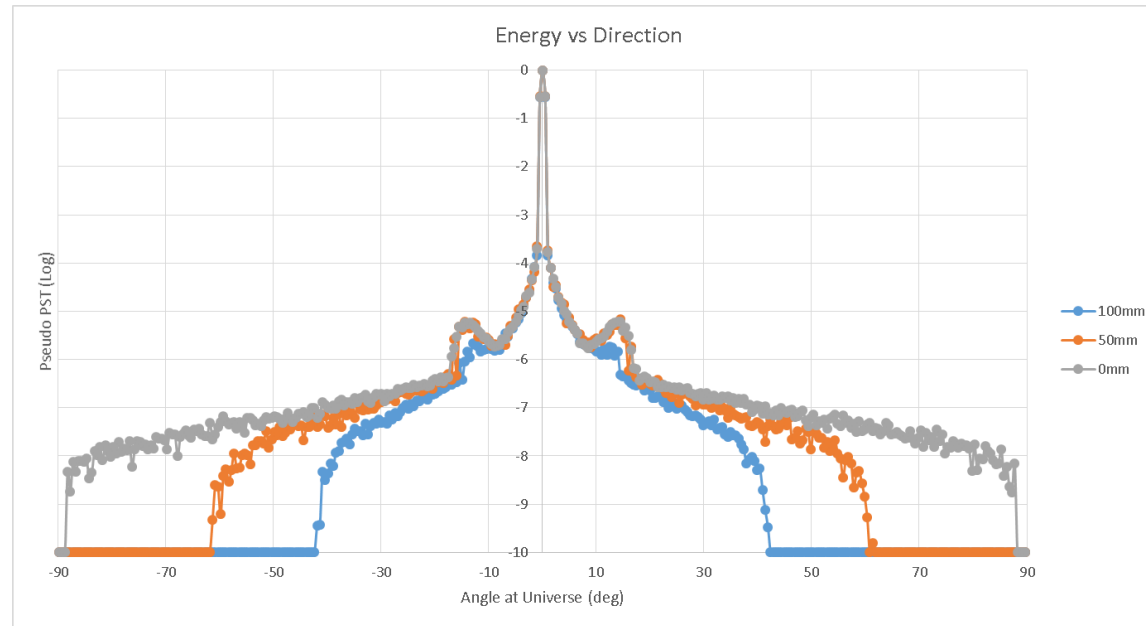
- The source irradiance at normal incidence is typically set to unity.
- This PST can be used as a transfer function: the total amount of light (stray or otherwise) reaching the focal plane is

$$P_{det}(\theta, \phi) = E_{inc}(\theta, \phi) \cdot PST(\theta, \phi) \cdot A_{det}$$

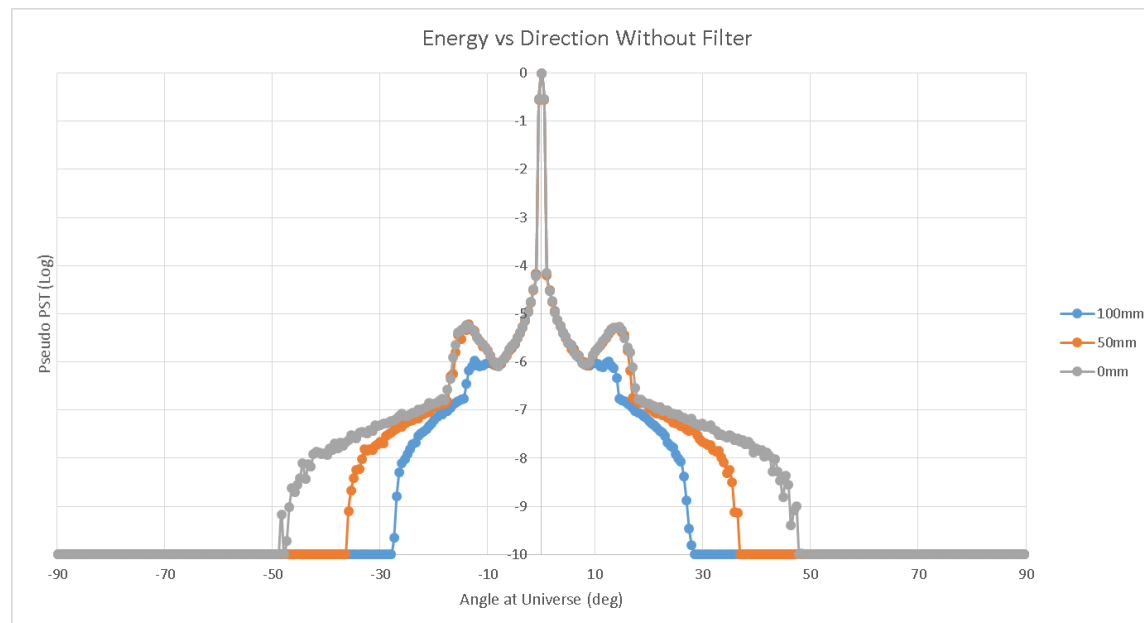


Effect of extended baffles and filter on PST

With Filter



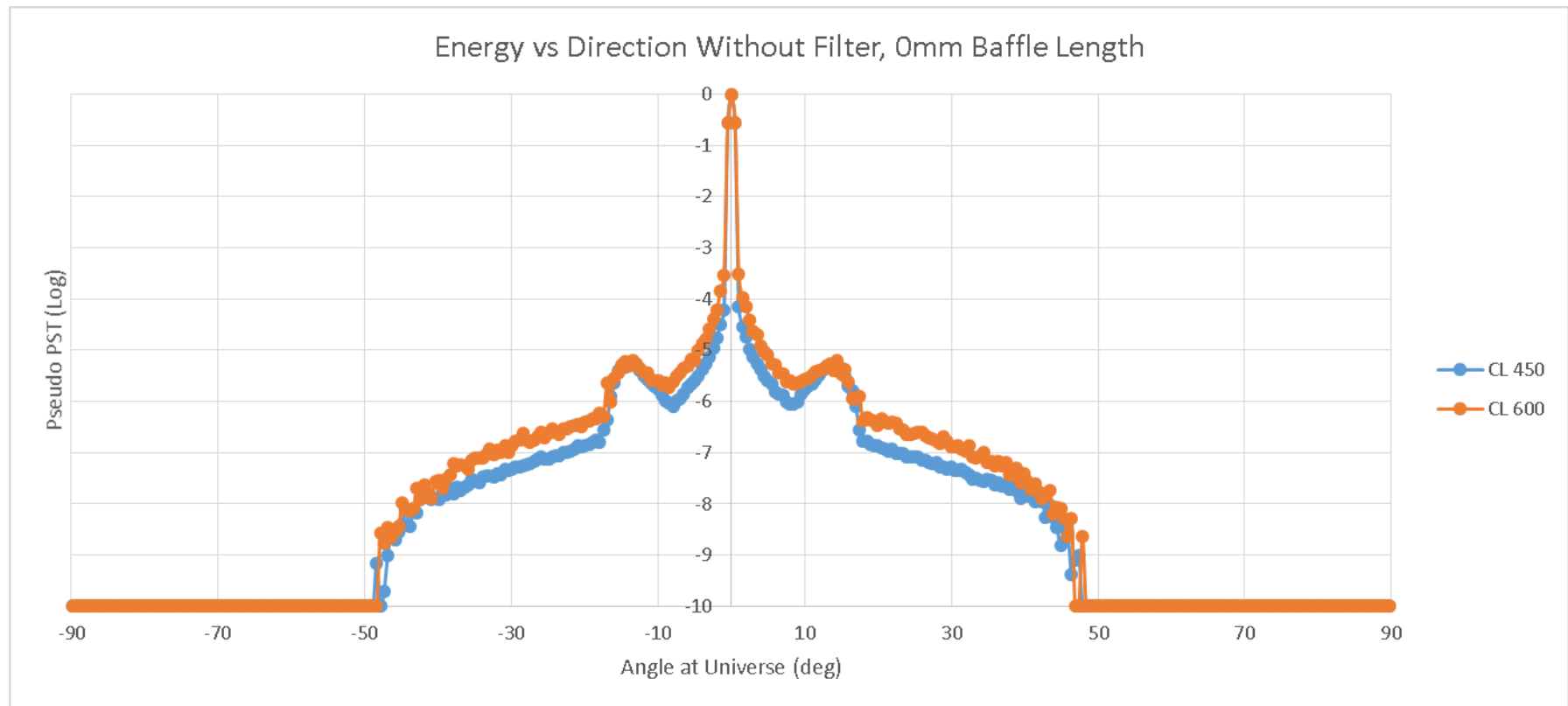
Without Filter





Contamination effect on the PST

- **Percent Area Coverage (PAC) = percent of surface which is obscured by particulates**
- **CL 450 = 0.164 PAC**
- **CL 600 = 0.696 PAC**





Manufacture tolerances

3D decenter of Detector: 0.5 mm

3D decenter of mirror: 2.0 mm

Mirror focal length 1.0 mm

Mirror tip/tilt: 0.05 rad

Detector tip/tilt: 0.05 rad



Scatter model

- Empirically derived from measurement
- No intrinsic wavelength dependence
- Lorentzian around specular ray
- **Linear-shift invariant: BSDF** depends on the difference $(\beta - \beta_0)$ between the specular and scattered rays

Harvey-Shack

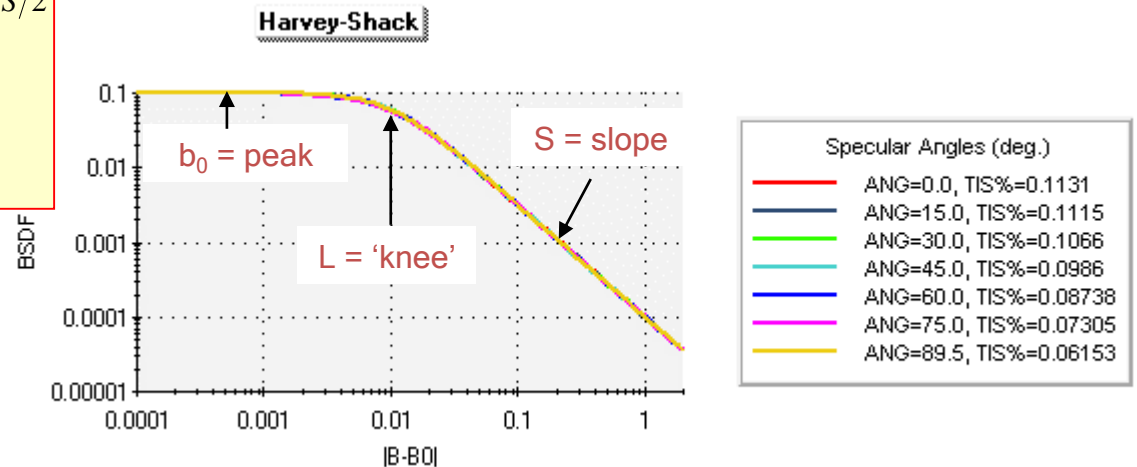
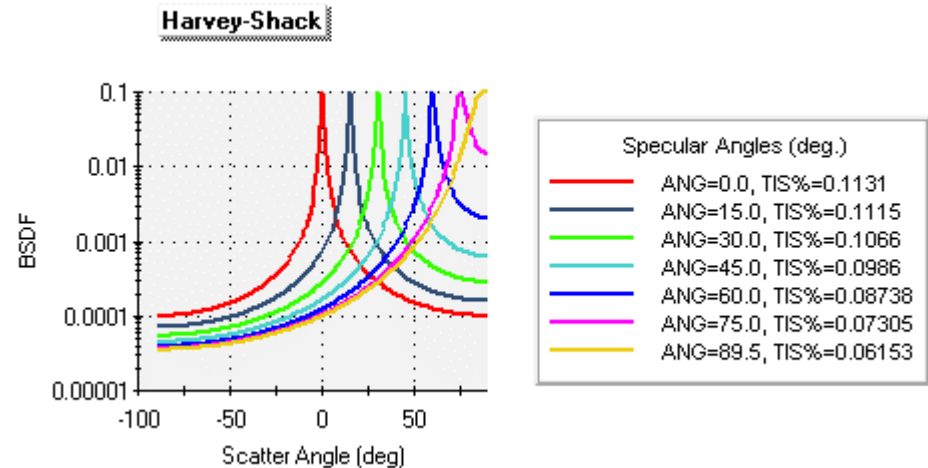
$$BSDF(\beta, \beta_0) = b_0 \left(1 + \left(\frac{\beta - \beta_0}{L} \right)^2 \right)^{S/2}$$

specular peak = b_0

ABg

$$BSDF(\beta, \beta_0) = \frac{A}{B + (\beta - \beta_0)^g}$$

specular peak = A/B

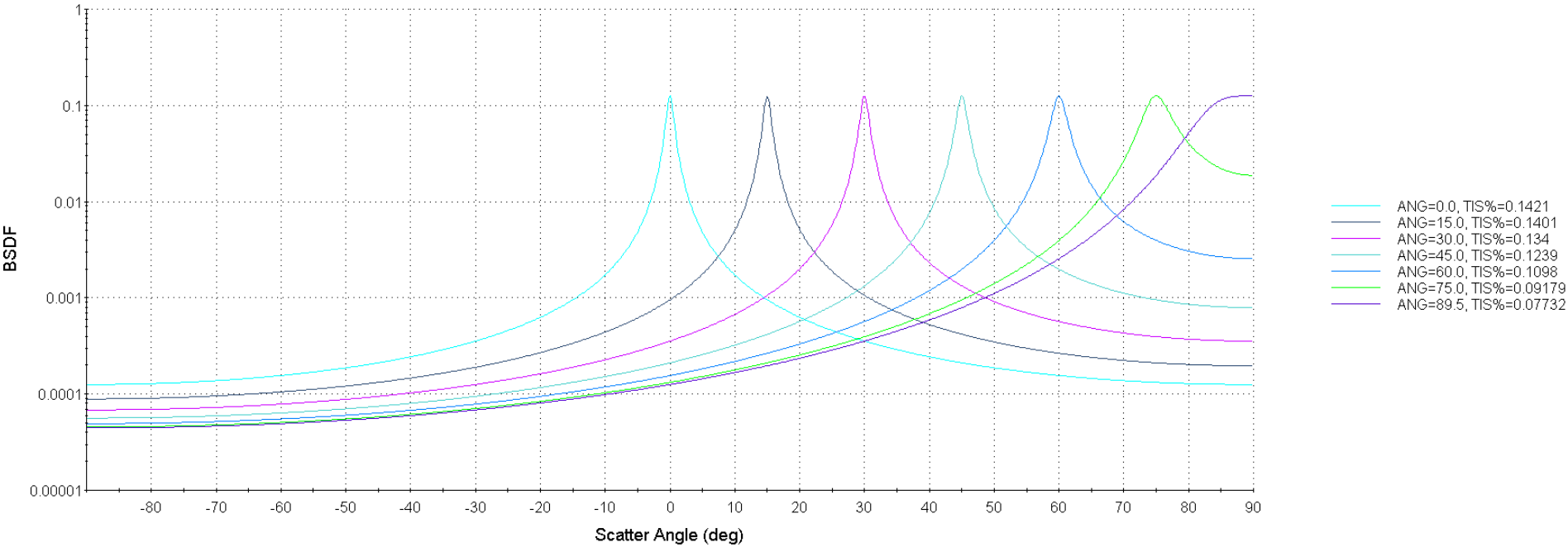




Scatter model

Mirror 30Å Surface Roughness

BSDF Scatter Plot

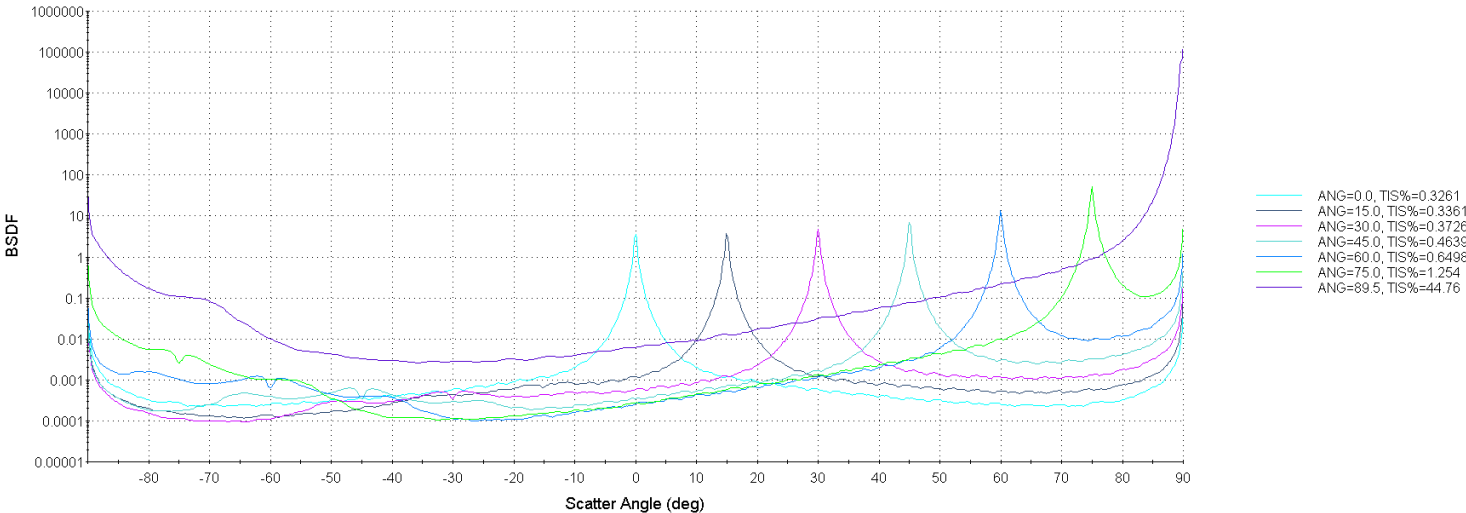




Scatter model

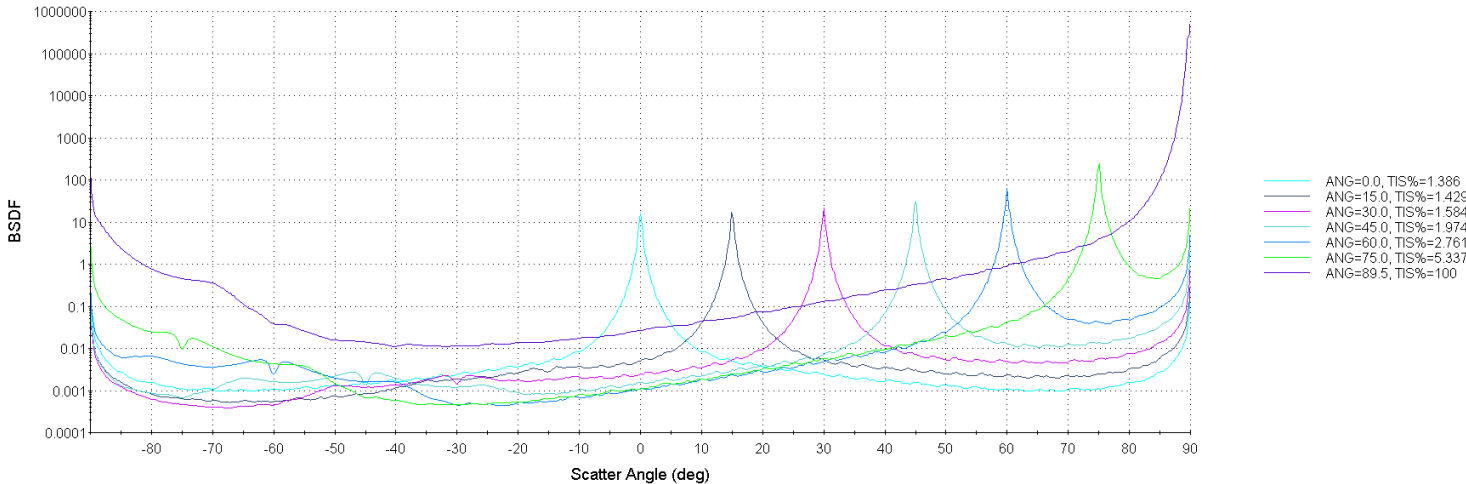
Mirror Particulates CL450

BSDF Scatter Plot



Mirror Particulates CL600

BSDF Scatter Plot

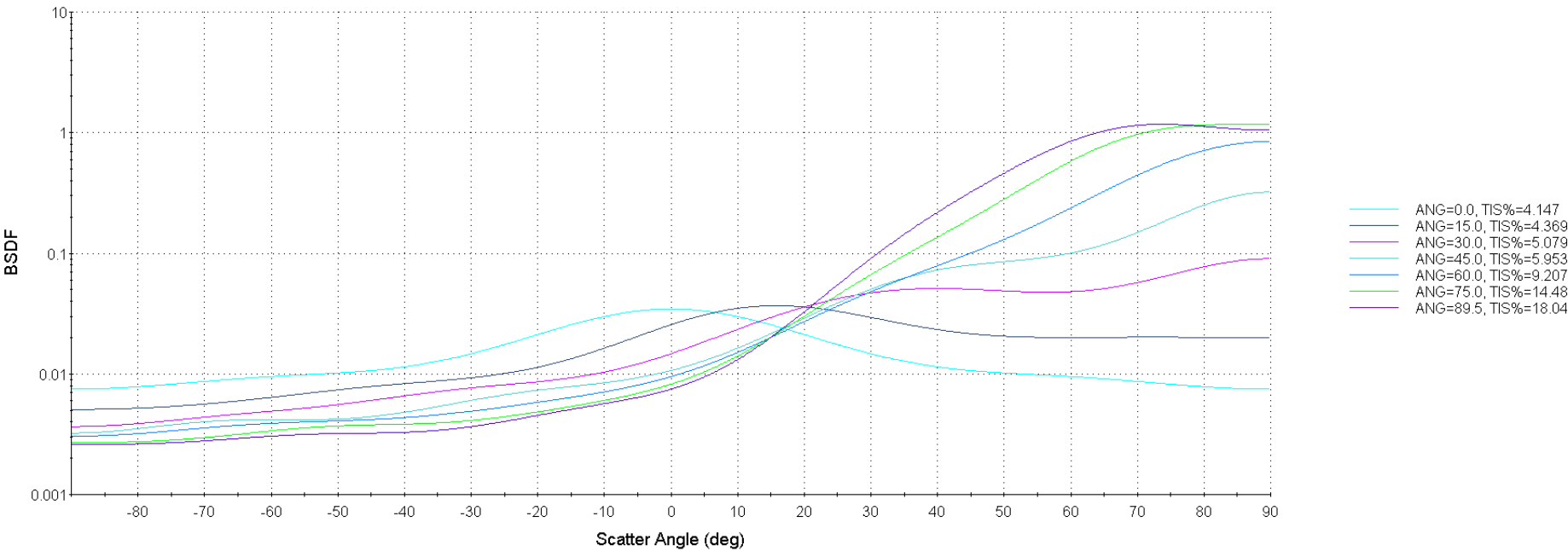




Scatter model

Z306 Diffuse Black Paint

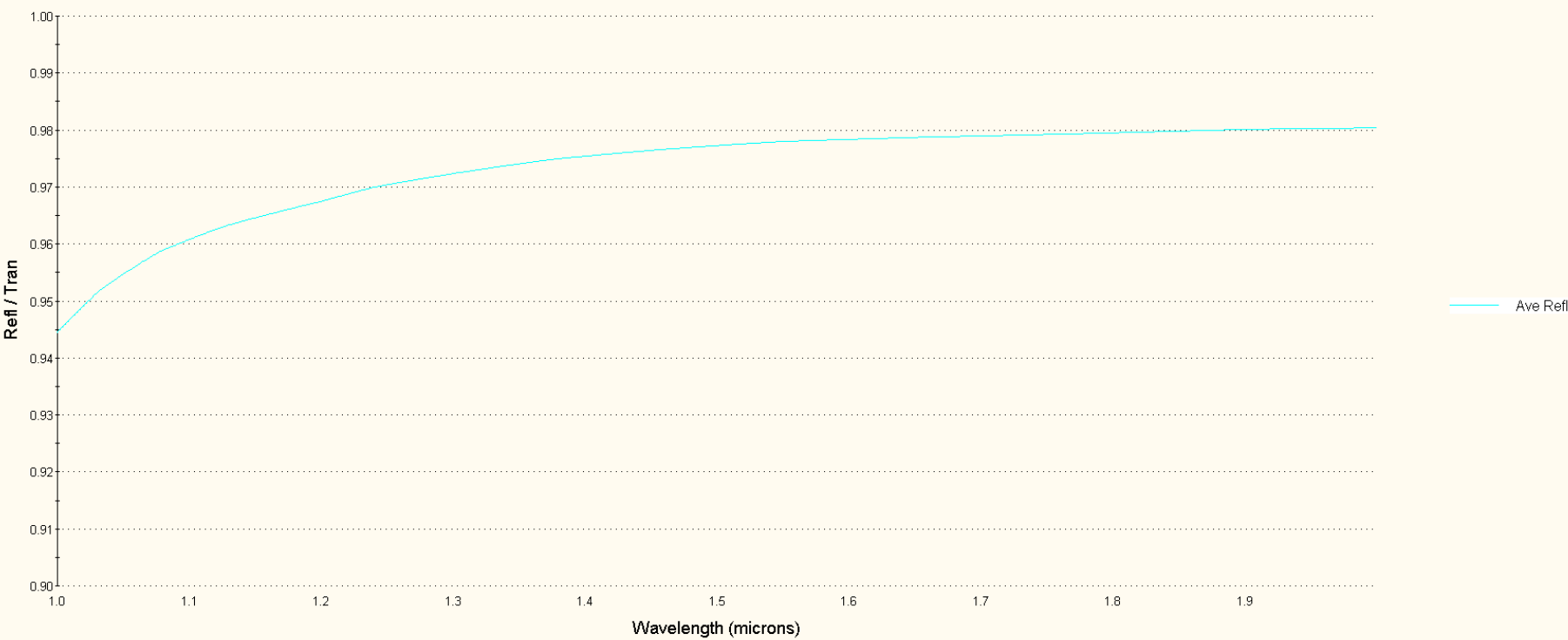
BSDF Scatter Plot





Bare Al Coating (Mirror) - Reflectivity

"Al_Mirror" coating at 0.0000 deg AOI



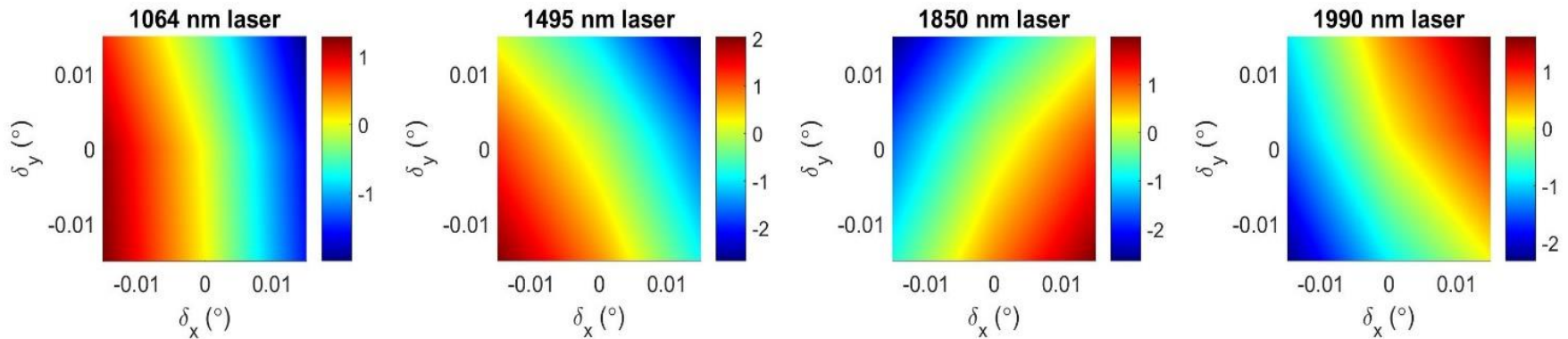


Systematic errors due to pointing instabilities

$$P_{detected,\lambda} = P_{emitted,\lambda} \times R_{\lambda} \times \int PST_{\lambda}(\theta_x - \delta_x, \theta_y - \delta_y) LDP_{\lambda}(\theta_x, \theta_y) d\theta_x d\theta_y$$

$$SE(\%) = \frac{\int PST_{\lambda}(\theta_x, \theta_y) LDP_{\lambda}(\theta_x, \theta_y) d\theta_x d\theta_y - \int PST_{\lambda}(\theta_x - \delta_x, \theta_y - \delta_y) LDP_{\lambda}(\theta_x, \theta_y) d\theta_x d\theta_y}{\int PST_{\lambda}(\theta_x, \theta_y) LDP_{\lambda}(\theta_x, \theta_y) d\theta_x d\theta_y} \times 100$$

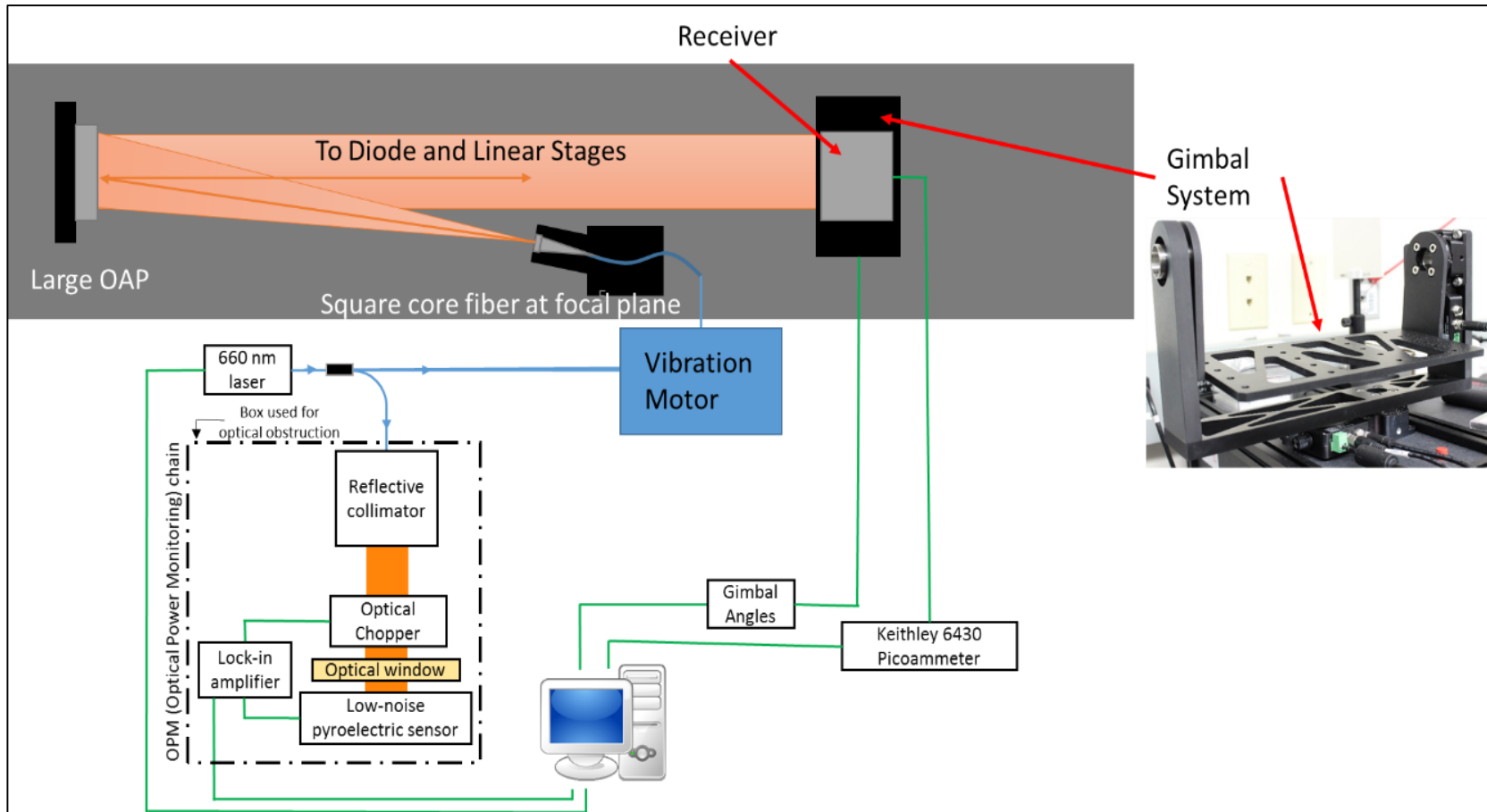
$$\Delta = \max \left[\left| \frac{\int PST_{\lambda}(\theta_x, \theta_y) LDP_{\lambda}(\theta_x, \theta_y) d\theta_x d\theta_y - \int PST_{\lambda}(\theta_x - \delta_x, \theta_y - \delta_y) LDP_{\lambda}(\theta_x, \theta_y) d\theta_x d\theta_y}{\int PST_{\lambda}(\theta_x, \theta_y) LDP_{\lambda}(\theta_x, \theta_y) d\theta_x d\theta_y} \times 100 \right| \right]_{\forall \sqrt{\delta_x^2 + \delta_y^2} \leq AS}$$





Characterization and Calibration

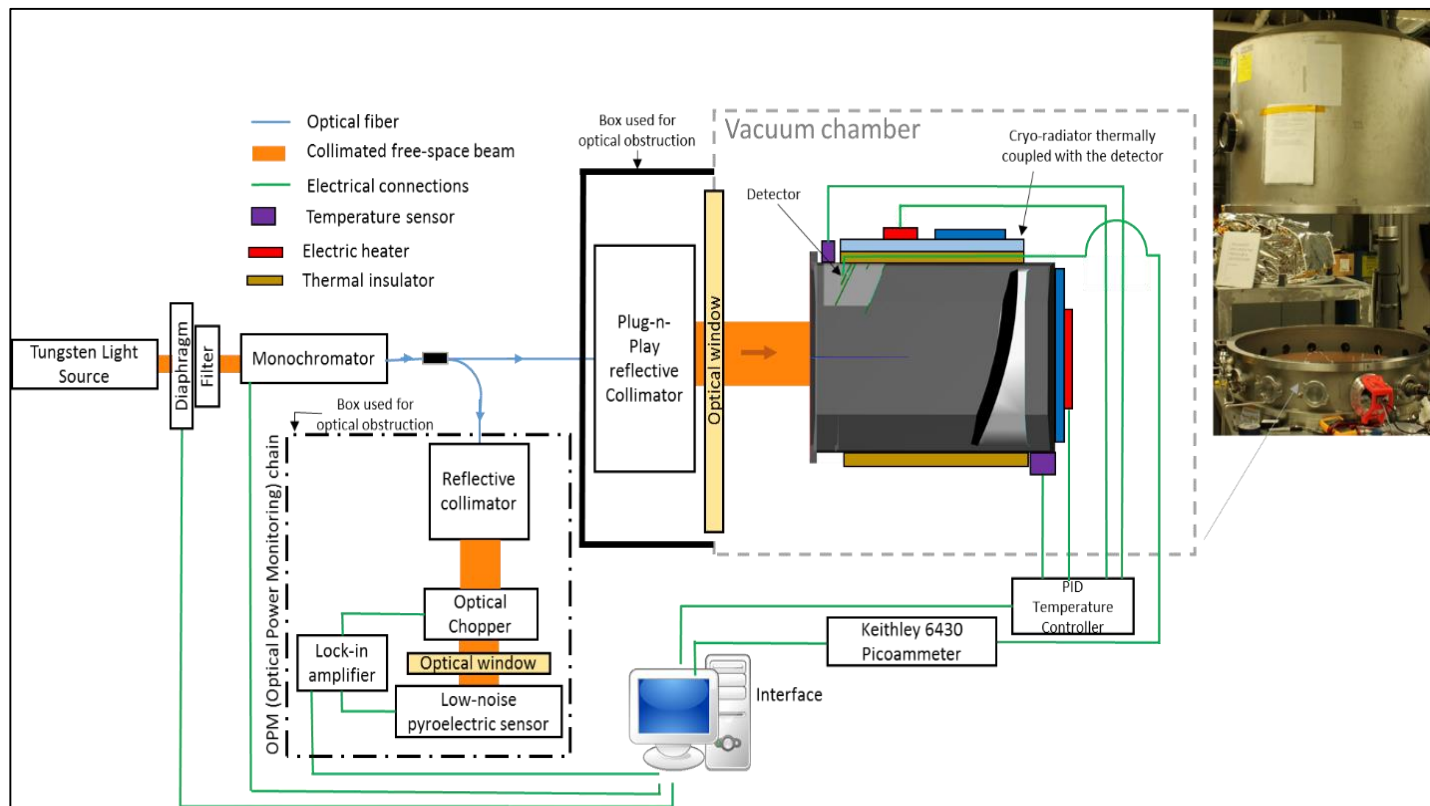
➡ PST VS incidence angles at room temperature





Characterization and Calibration

- ➔ Receiver responsivity VS wavelength, detector temperature and mirror temperature
- ➔ Detector bias current VS detector temperature and mirror temperature



Characterization/calibration conditions :

- Optical power at the receiver aperture: [20, 85] nW
- Operating temperature of the detector: -65 °C
- Operating temperature range of the receiver structure: [-65,7] °C
- Vacuum of 10^{-5} Torr